

Hao LUO, Mancang LI, Shanfang HUANG, Minyun LIU, Kan WANG

# Optimization of spatial structure designs of control rod using Monte Carlo code RMC

© Higher Education Press 2021

**Abstract** Control rod is the most important approach to control reactivity in reactors, which is currently a cluster of pins filled with boron carbide ( $B_4C$ ). In this case, neutrons are captured in the outer region, and thus the inner absorber is inefficient. Moreover, the lifetime of the control rod is challenged due to the high reactivity worth loss resulted from the excessive degradation of  $B_4C$  in the high flux area. In this work, some control rod designs are proposed with optimized spatial structures including the spatially mixed rod, radially moderated rod, and composite control rod with small-sized pins. The control rod worth and effective absorption cross section of these designs are computed using the Monte Carlo code RMC. A long-time depletion calculation is conducted to evaluate their burnup stability. For the spatially mixed rod, rare-earth absorbers are combined with  $B_4C$  in spatial structure. Compared with the homogenous  $B_4C$  rod, mixed designs ensure more sufficient reactivity worth in the lifetime of the reactor. The minimum reactivity loss at the end of the cycle is only 1.8% from the dysprosium titanate rod, while the loss for pure  $B_4C$  rod is nearly 12%. For the radially moderated design, a doubled neutronic efficiency is achieved when the volume ratio of moderator equals approximately 0.3, while excessive moderating may lead to the failure of control rods. The control rod with small-sized pins

processes an enhanced safety performance and saves the investment in absorbers. The rod worth can be further enhanced by introducing small moderator pins, and the reactivity loss caused by the reduction of absorbers is sustainable.

**Keywords** control rod, optimized spatial structure, neutronic performance, burnup stability

## 1 Introduction

Control rod is an essential part of the reactor reactivity control system. The new generation nuclear power plants (NPPs) require control rods to play a more critical role in reactivity compensation, power distribution regulation, and reactor shutdown [1]. In the AP1000 reactor developed by Westinghouse, an advanced control system, designated MSHIM (mechanical shim), was employed for simultaneous reactivity control without adjusting the soluble boron concentration [2]. In fast reactors and many research reactors, control rods are frequently inserted and withdrawn in the lifetime of the reactor [3,4]. Long-time neutron irradiation will cause severe radiation damage to control rods, resulting in a decline of the reactivity control ability and seriously affecting the neutronic life of the control rods [5,6].

To extend the neutronic lifetime and improve the neutronic efficiency, in recent years, extensive research on the spatial structure of the control rods has been conducted. Westinghouse adopted an axially layered design in AP1000 control rods, using  $B_4C$ , Ag-In-Cd, and stainless steel as absorbers in the axial direction [7]. General Electric Hitachi also used hafnium and  $B_4C$  as absorbers, respectively in the top and bottom segments of the control rod blades in boiling water reactors (BWRs) because different element receives different neutron fluences [7]. To improve the neutronic efficiency, Devan et al. [8] used  $B_4C$  absorber with different  $^{10}B$  enrichment in the axial direction of the control rod. Without

Received Dec. 28, 2020; accepted May 7, 2021; online Sept. 30, 2021

Hao LUO, Shanfang HUANG (✉), Kan WANG  
Department of Engineering Physics, Tsinghua University, Beijing 100084, China  
E-mail: sfhuang@tsinghua.edu.cn

Mancang LI  
Science and Technology on Reactor System Design Technology Laboratory, Nuclear Power Institute of China, Chengdu 610213, China

Minyun LIU  
CNNC Key Laboratory on Nuclear Reactor Thermal Hydraulics Technology, China National Nuclear Corporation Nuclear Power Institute of China, Chengdu 610213, China

Special Issue: Innovative Nuclear Energy Technology

compromising on the requirements of the control rod worth, the consumption of enriched  $^{10}\text{B}$  was reduced.

Moreover, due to the spatial self-shielding [9], the inner absorbers are less effective than the outer ones. Thus, absorption capabilities are always overestimated. To improve neutronic efficiency, Japan research reactor (JRR-3) [10] and China Advanced Research Reactor (CARR) [11] both utilized a radially hollow control rod structure. For the same reason, a small pin control rod design was adopted in sodium fast reactors (SFRs) [12]. Furthermore, moderate materials were also applied to optimize the utilization of the absorbers and improve the absorption ability [13–15]. Although research on the spatial structure optimization of control rod is in full swing, related designs should be assessed in-depth on the neutronic efficiency and burnup stability under long-term irradiation. In addition, more innovative control rod designs need to be investigated.

In this paper, the optimal designs for control rod in spatial structure is conducted in the JRR-3 research reactor. The Monte Carlo code RMC [16] is used for neutronic simulation and long-time burnup calculation. Optimized control rod models with different spatial structures are established, such as spatially mixed control rod, radially moderated control rod, and composite control rod with small-sized pins. To assess the performance of these designs, the control rod worth (CRW), effective absorption cross section (EACS), and burnup stability are computed.

## 2 Depletion simulation and optimized designs of control rod

### 2.1 Modeling and depletion simulation of control rod

The objective of this work is to establish innovative control rod designs with different spatial structures. Conceivably, related models may exhibit complex layouts, and the flux gradient in control rod is also intricate, which requires accurate modeling and precise depletion calculation. Monte Carlo (MC) burnup calculations are feasible for this objective by combining MC transport calculation and point-burnup calculation. Some of the MC codes, such as MCNP [17], OPENMC [18], SERPENT [19], MCB [20], and MVP-BURN [21], have built-in burnup module or couple with the depletion code, e.g., ORIGIN-2 [22]. This work employs the Monte Carlo code RMC for the optimal designs for its ability to deal with complex geometry [16] and handle detailed depletion chain [23]. Moreover, RMC code has the large-scale reactor burnup calculation function, which has already been implemented and benchmarked [24,25], and thus is a good solution for this research.

In the process of control rod modeling, considering the “skin” effect, the deterministic method uses spatial meshes (see Fig. 1(a)) and the homogenized cross section [26,27].

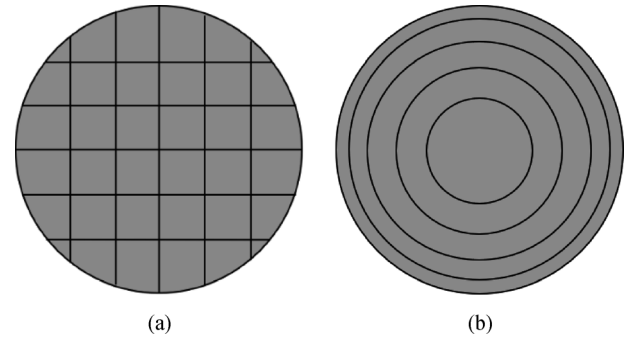


**Fig. 1** Sub-burnup cell divided strategy.  
(a) Deterministic method; (b) stochastic method.

In the stochastic MC method, as shown in Fig. 1(b), the control rod is divided into multiple equal-volume sub-burnup cells. Obviously, more sub-burnup cells are beneficial to solve the self-shielding effect but will increase the statistical fluctuation of neutronics parameters, such as the flux and absorption cross section. Consequently, in this work, the control rod is divided into five sub-burnup cells for high-fidelity depletion calculation.

For control rod depletion calculation, the capture energy of absorbing isotope is utilized in the process of power distribution, which is beneficial for the meticulous simulation. Then, the neutron flux of each control rod cell is computed using the “const power mode” [28]. For solving burnup equations, RMC utilizes the Chebyshev rational approximation method (CRAM) [29] for its good robustness and high computational efficiency. It is noticed that the burnup data library using in RMC includes 1487 isotopes, while there are only about 300 isotopes in ACE data library. As a result, the nuclides will be selected according to the absorption reaction rate and atomic density after burnup calculation, and then added to burnup cell materials for transport calculation of the next burnup step.

Moreover, a “frozen fuel” strategy is adopted for the control rod depletion simulation. This methodology was first proposed by Franceschini et al. [30], which means only the control rod is allowed to deplete. Figure 2 shows the detailed framework of the “frozen” fuel strategy coupled with the RMC control rod depletion module. To meet the “frozen” fuel requirements, fissionable materials are initialized at the end of every burnup step, and the absorbers in control rod cells continue to deplete. Therefore, the flux in control rods and the absorption cross section vary only owing to the transmutation of absorbing materials. This enables an assessment on neutronic and burnup performance of different control rods due to the degradation of absorbers only, and without the effect of fuel depletion.

### 2.2 Optimization design direction

Before optimization, the defects of the traditional control

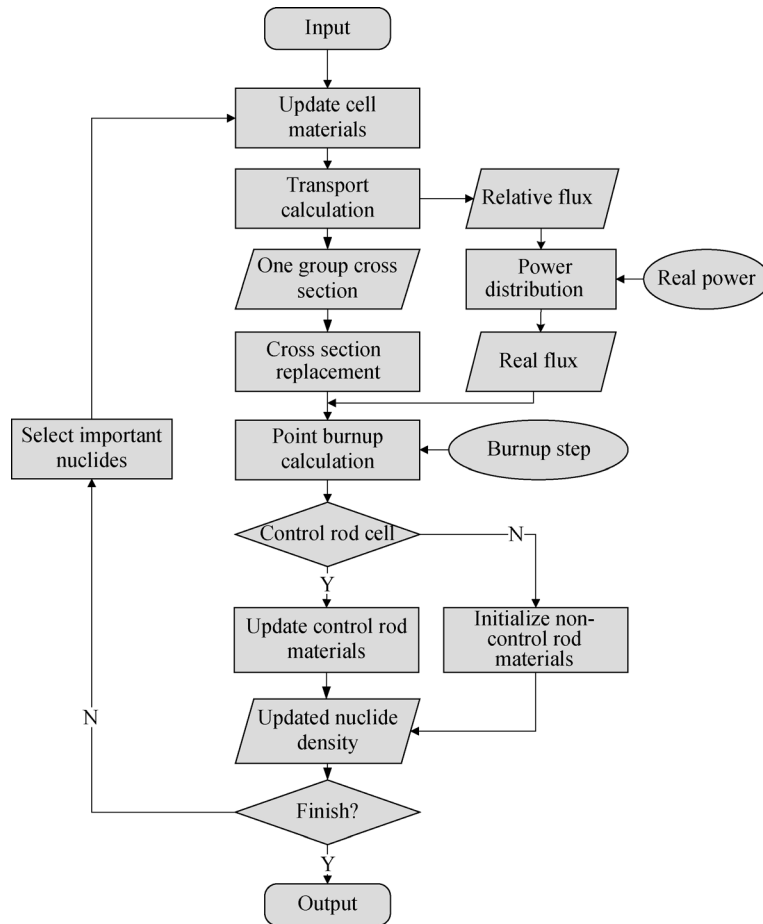


Fig. 2 Framework of depletion model of control rod.

rod in the spatial structure need to be clarified. A cylindrical  $B_4C$  control rod (see Fig. 3) with a clad outer diameter of 7 cm and an absorber diameter of 5.8 cm is constructed to estimate the neutronic parameters, such as flux, absorption rate and cross section, absorbing material depletion rate, etc. Figure 4 gives the  $^{10}B$  depletion rate in different axial regions of the  $B_4C$  control rod in one year. The absorbers in the central area are excessively depleted under higher neutron flux irradiation, resulting in the loss of control rod worth. Besides, the swelling caused by the helium release from the  $(n,\alpha)$  reaction of  $^{10}B$  may lead to a severe pellet-cladding mechanical interaction (PCMI) [31]. Severe radiation damage may lead to the failure of the control rod.

The traditional  $B_4C$  control rod is also inefficient in neutronic performance. As demonstrated in Fig. 5, the flux and absorption rate decrease from the outer to the inner region, and there are distinct gradients in the effective absorption cross section of the control rod, which reflects the self-shielding effect. In this case, the outer absorber is more efficient than the inner one, and the absorption ability of the control rod may be overestimated.

### 2.3 Innovative control rod designs

Based on the calculation strategy mentioned in Section 2.1 and the optimization direction in Section 2.2, the innovative spatial structure designs and detailed control rod modeled in RMC are proposed in this Section. Based on the traditional  $B_4C$  control rod, the optimized spatial structure designs of the control rod presented herein includes spatially mixed control rods, radially moderated control rods, and composite control rods with small-sized pins.

#### 2.3.1 Spatially mixed control rods

In the modeling of the two spatially mixed control rods, hafnium hydride [32], dysprosium titanate [33], and europium oxide [34] are introduced to substitute  $B_4C$ . These rare-earth absorbers capture neutrons by the  $(n,\gamma)$  reaction without gas production, which can avoid the PCMI phenomenon. Besides, the rare-earth absorbers and their depletion products have a neutron absorbing capability with a considerable absorption cross section.

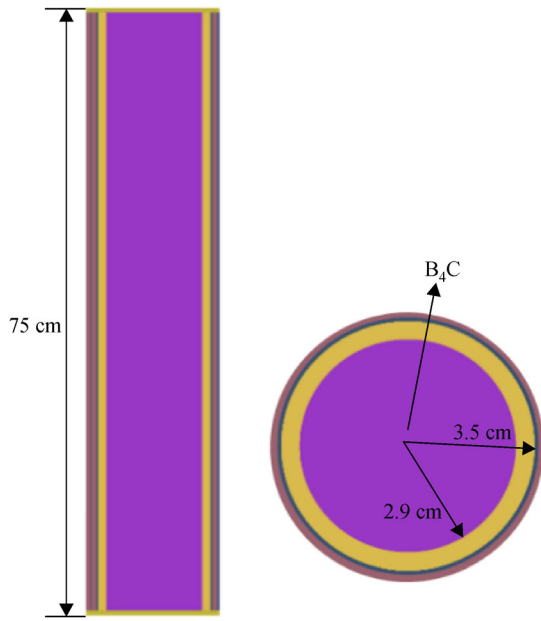


Fig. 3 Layout of traditional control rod.

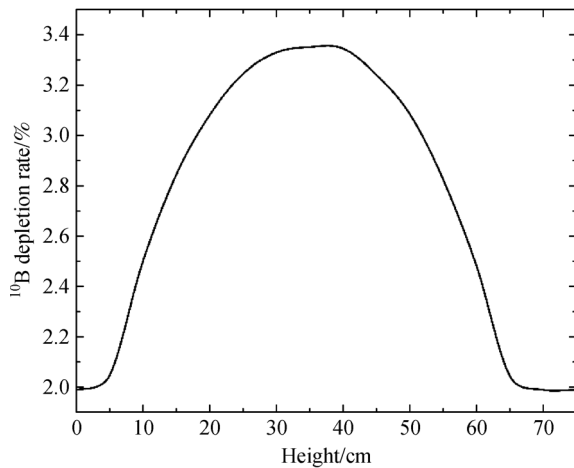


Fig. 4 <sup>10</sup>B depletion rate of different axial region in one year.

Consequently, the burnup stability is expected to be more excellent than that of the B<sub>4</sub>C control rod.

Figure 6(a) exhibits the axially partitioned control rod design. Considering the higher neutron flux in the central region and the characteristics of the absorbers mentioned in Section 2.2, axially partitioned control rod is designed with hafnium hydride, dysprosium titanate, and europium oxide in the top portion of the absorber column, and the remaining part by the B<sub>4</sub>C absorber.

Similarly, the spatial self-shielding effect (see Section 2.2) indicates that the inner absorbers are less efficient than the outer ones. To minimize the self-shielding effect and make full use of the absorbing characteristics of different materials, as Fig. 6(b) illustrates, a structure described as “weak outside and strong inside” is adopted. In this structure, the B<sub>4</sub>C with a large neutron absorption cross-section is arranged in the inner region, and the rare-earth absorbers are arranged in the outer region for their longer burnup chain. During the irradiation process, it is expected that the daughter nuclides of the outer rare-earth absorber with a neutron absorbing capacity can inherit the absorption capacity and thus extend the neutronic lifetime of the control rod. Meanwhile, the inner B<sub>4</sub>C can keep a high neutron absorbing capacity for its large cross section without losing its reactivity worth. Since B<sub>4</sub>C is still utilized in this design, an air gap is set between the absorber pellet and the clad to avoid their direct interaction, and thus the control rod failure caused by the PCMI phenomenon can nearly be avoided.

### 2.3.2 Radially moderated control rods

Based on the radially mixed design, to maximize the neutronic efficiency and minimize the spatial self-shielding effect in the control rod, a radially moderated control rod design is proposed as depicted in Fig. 6(c). In this design, a radially mixed control rod is assumed in which the moderator replaces the inner absorber. It is expected that the moderator can enhance the local neutron flux, and consequently, the same CRW can be achieved with fewer absorbers. However, the decrease of the absorber and the increase of the moderator will simultaneously affect the

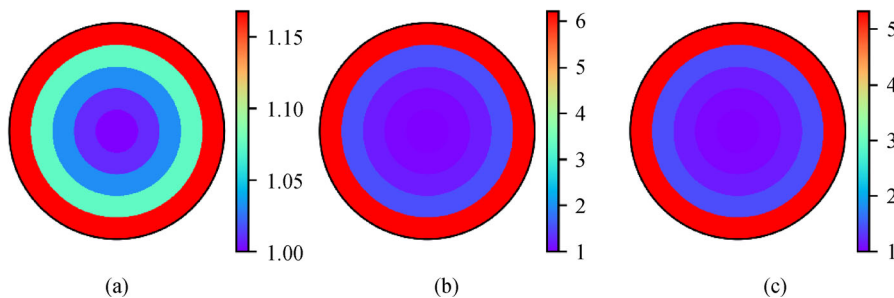
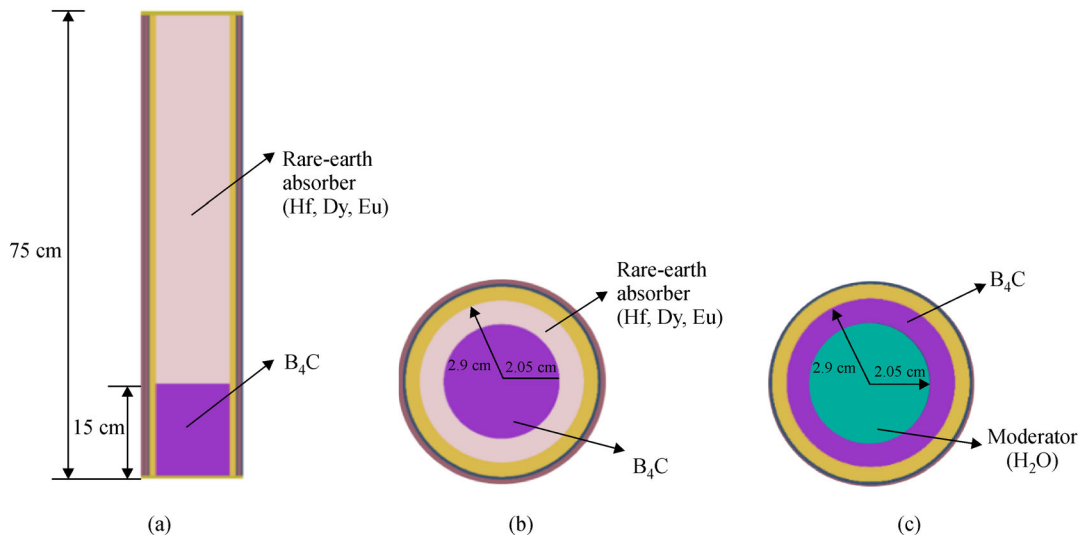


Fig. 5 Neutronic parameters of control rod in radial direction. (a) Flux (neutron/cm<sup>2</sup>·s); (b) absorption rate (neutron/s); (c) effective absorption cross section (cm<sup>-1</sup>).



**Fig. 6** Layout of spatially mixed control rods.  
(a) Axially partitioned rod; (b) radially layered rod; (c) radially moderated rod.

characteristics of the control rod. Thus, control rods with different proportion of the moderator need to be investigated.

As for the chosen of the moderator, in this paper, water is utilized for its cooling and moderating capability in JRR-3. For reactors that do not use water as coolant, such as sodium fast reactors (SFR) and gas-cooled fast reactor (GFR), according to Ref. [15], numerous moderators, such as  $ZrH_2$ ,  $BeO$ ,  $LiH$ , etc. are all potential candidates for their promising moderating properties.

### 2.3.3 Control rod with composite small-sized pins

From the perspective of reactor safety, the control rod system is required to provide sufficient reactivity control during the whole reactor lifetime. The increasing numbers of operating control rods will reduce the possibility of a severe accident caused by a single control rod failure. Besides, the large-sized control rod has defects in utilization efficiency, irradiation properties, and mechanical strength. As a result, a control rod with small-sized pins that is feasible in reducing the spatial self-shielding effect and improving efficiency is proposed. The layout of control rods with different numbers of small-sized pins is described in Fig. 7(a) and detailed design dimensions of these designs are given in Table 1. In this design, more small-sized absorber pins are adopted to replace the one big-sized pin and the gap between the pins is filled with helium.

This design will also increase the flexibility of reactivity control. As Fig. 7(b) shows, moderator pins are utilized to help smoothen the neutron flux and increase the absorption cross section of surrounding absorber pins. Also note that, in this design, the moderator material adopts  $ZrH_2$  for its

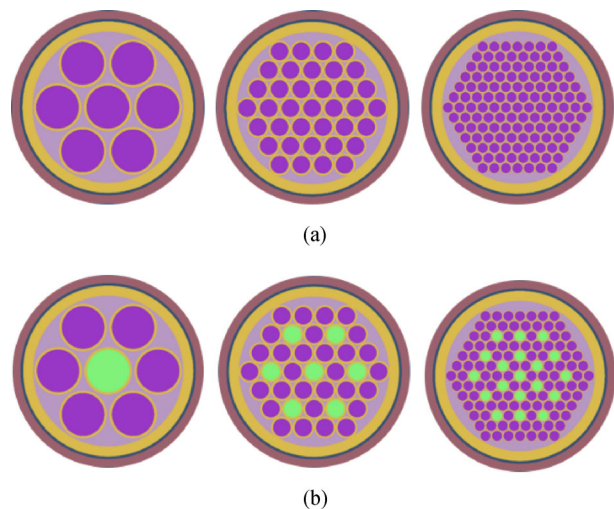


**Fig. 7** Control rods with small-sized pins.  
(a) All absorber pins; (b) absorber and moderator pins.

metal characteristics.

## 2.4 Optimization carrier

The optimized design of control rods adopts the JRR-3 research reactor as carrier, which has been operating safely since 1962 [10]. There are six control rod assemblies and 20-six fuel assemblies, and the control rod is the only reactivity control system. In this case, the computing results of different control rods can reflect their own neutronics characteristics. The detailed design parameters of JRR-3 are given in Table 2.

In this work, the cylindrical control rods and  $B_4C$  material are applied to substitute the original design for

**Table 1** Detailed dimensions of composite control rods

Composite control rods	Pin number	Clad radius/cm	Pin absorber radius/cm	Pin material
Absorber pins	7	0.95	0.85	B <sub>4</sub> C
	37	0.45	0.35	
	127	0.23	0.2	
Absorber and moderator pins	6 + 1	0.95	0.85	B <sub>4</sub> C and ZrH <sub>2</sub>
	30 + 7	0.45	0.35	
	108 + 19	0.23	0.2	

**Table 2** Main design parameters of JRR-3 core [10]

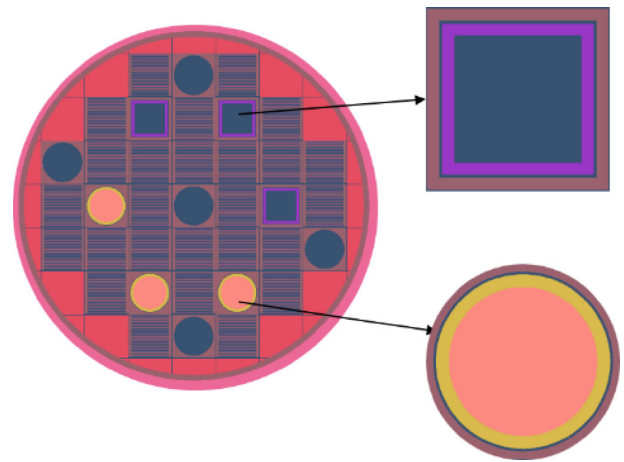
Parameter	Value
Reactor power/MW	20
Active core height/cm	75
Active core radius/cm	53
Fuel assembly type	Plate
Fuel plate number	20
Fuel meat material	U <sub>2</sub> Si <sub>3</sub>
U density/(g·cm <sup>-3</sup> )	3.8
<sup>235</sup> U enrichment	19.75
Absorber thickness/cm	0.8
Meat thickness/cm	0.076
Meat width/cm	6.16
Cladding thickness/cm	0.038
Cladding width/cm	0.48
Moderator gap width/cm	0.228
Control rod type	Hollow frame
Absorber material	Hf
Clad thickness/cm	1
Gap in control rod/cm	0.26

their extensive application and versatility. The JRR-3 core and the two control rods modeled in RMC are displayed in Fig. 8.

### 3 Results and discussion

In the realistic operation scenario, control rods are inserted or withdrawn frequently to compensate for the reactivity loss. However, following the exact operation history of the control rod movements poses challenge to numerical simulation. Practically, in this study, control rods are supposed to be fully inserted while fuels are kept fresh. For an in-depth comparison and assessment, the irradiation time of all control rods is extended to 20 years under the maximum power 20 MW of the JRR-3 reactor.

The ENDB-VIII.0 nuclear data library is employed for the RMC criticality and burnup calculation, and 50000

**Fig. 8** Layout of JRR-3 core, hollow control rods and new cylindrical rods.

particles per cycle are used and 250 active and 50 inactive cycles are adopted. Specific designs and the expectations have been discussed in Section 2.3, and detailed analysis on neutronic characteristics and burnup stability will be presented below.

#### 3.1 Control rods with different absorbers in axial and radial direction

The first set of assessments is the neutronic performance of the mixed control rods, including absorption cross section and control rod worth, which can be calculated as [35,36]

$$CRW = \rho_{out} - \rho_{in} = \frac{k_{out} - k_{in}}{k_{out} \cdot k_{in}},$$

where  $\rho$  and  $k$  are reactivity value and effective multiplication, and the subscript in and out mean that control rods are completely inserted and withdrawn. The effective multiplication factor  $k_{out}$  at the beginning of cycle (BOC) is 1.242.

As listed in Table 3, taking the pure B<sub>4</sub>C control rod as a reference, the HfH<sub>1.3</sub> control rod has the biggest reactivity worth, and the enhancement of effective absorption cross section is about 38.9% among these three control rods. The rod worth of Eu<sub>2</sub>O<sub>3</sub> is comparable to that of the pure B<sub>4</sub>C

rod, while the  $Dy_2TiO_5$  rod has a lower worth since the absorption cross section of dysprosium is relatively small. The standard deviations of all calculation results are also given in Table 3.

The burnup performance of these mixed control rods is then evaluated by computing the CRW at each burnup step. The relative CRW curve (see Fig. 9) reflects the burnup stability of different control rods. It is shown that the  $Dy_2TiO_5$  rod surpasses all other rods in burnup stability. Its reactivity loss at the end of the cycle (EOC) is only 1.8%, while the maximum reactivity loss is approximately 12.8% for the  $B_4C$  rods. Since the rare-earth elements have a longer depletion chain than  $B_4C$ , the improvement on keeping the reactivity control ability of these axially mixed control rods is quite significant.

Benefitting from the great neutron absorbing capacity of the daughter nuclides, similar calculation results for radially layered control rods are obtained and listed in Table 4. The hafnium and europium control rods have a less reactivity loss of about 8.7% and 4.4% at EOC while keeping the absorbing capacity at BOC. Simultaneously, although the dysprosium control rod is disadvantageous in the neutron absorbing ability at BOC, it is more exceptional in the burnup stability with only a 7.9% loss in the effective absorption cross section at EOC. Similar to criticality calculations, the standard deviations of burnup calculations are about  $7E-05$ .

### 3.2 Control rods with a moderator

The results given in Table 5 are in great agreement with the expectations about the radially moderated design in Section 2.3.2. As the proportion of moderator gradually increases, the moderated control rods have a higher neutron absorbing capacity and CRW. These new designs save the investment of absorbers and then significantly improve the neutronic efficiency. When  $R_m/R \approx 0.5$ ,

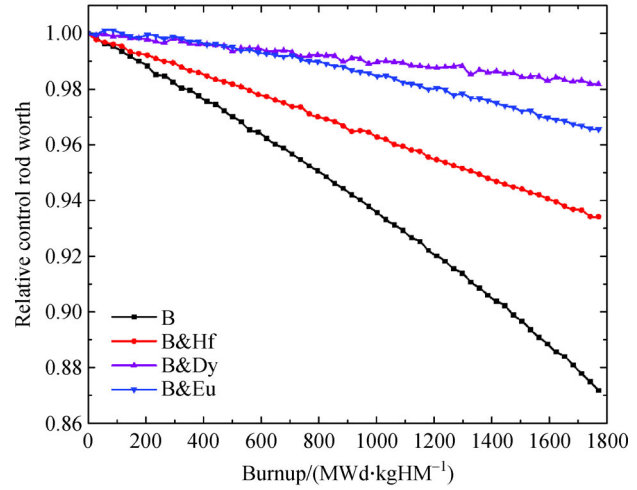


Fig. 9 Burnup performance of relative control rod worth.

the neutronic efficiency nearly doubled and when  $R_m/R \approx 0.7$ , there is an improvement of nearly four times, where  $R_m$  is the radius of moderator column and  $R$  is the radius of the control rod.

Nevertheless, the moderator improves the neutronic efficiency, but the total absorption cross section is not increased since part of the absorber is replaced. The effective absorption cross section decreases when the proportion of the moderator is over 0.3. Simultaneously, the use of the moderator significantly increases the reaction rate of the absorbers. The excessive consumption of the absorber in the moderated rod may lead to an unsustainable decrease in the burnup stability, especially for the  $B_4C$  absorber with a relatively short burnup chain.

As the burnup curve in Fig. 10 indicates, the control rod worth decreases with the consumption of  $^{10}B$ , and there are visible discrepancies of reactivity loss at EOC. In the most serious case, when  $R_m/R$  exceeds 0.89, the control rod

Table 3 Neutronic performance of axial partitioned control rod

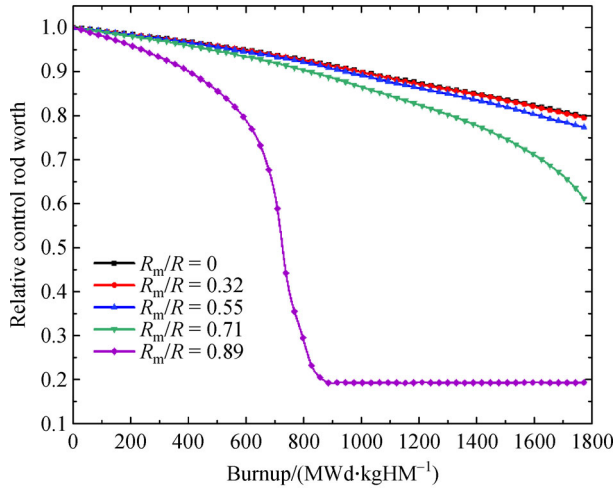
Absorber combination	$k_{eff}$	CRW/pcm	EACS/cm <sup>-1</sup>	$\sigma$
$B_4C$	1.038	15900	1.148E-01	8.0E-05
$B_4C$ and $HfH_{1.3}$	1.032	16400	1.594E-01	7.4E-05
$B_4C$ and $Dy_2TiO_5$	1.087	11500	6.844E-02	7.5E-05
$B_4C$ and $Eu_2O_3$	1.042	15500	1.222E-01	7.2E-05

Table 4 Burnup performance of radially layered control rods

Absorber combination	CRW at BOC/pcm	CRW at EOC/pcm	Loss/%	EACS at BOC/cm <sup>-1</sup>	EACS at EOC/cm <sup>-1</sup>	Loss/%
$B_4C$	15800	12600	20.2	1.15E-01	8.38E-02	27.0
$B_4C$ and $HfH_{1.3}$	15400	14100	8.7	1.16E-01	1.01E-01	13.5
$B_4C$ and $Dy_2TiO_5$	13400	12800	4.4	8.72E-02	8.03E-02	7.9
$B_4C$ and $Eu_2O_3$	15700	15000	4.4	1.22E-01	1.12E-01	8.4

**Table 5** Neutronic efficiency of different moderated control rods

$R_m/R$	$k_{eff}$	$\sigma$	CRW/pcm	CRW per unit mass absorber/(pcm·kg <sup>-1</sup> )	EACS/cm <sup>-1</sup>
0.89	1.028	7.6E-05	16800	33.7	8.72E-02
0.71	1.020	5.4E-05	17600	17.6	1.00E-01
0.55	1.020	7.5E-05	17500	7	1.19E-01
0.32	1.026	5.5E-05	17000	4.9	1.22E-01
0	1.033	8.0E-05	16300	3.6	1.19E-01



**Fig. 10** Relative CRW of moderated control rods changes with burnup.

worth drops sharply after about 3000 effective full power day (EFPD), which affects the safe operation of the reactor. Analyzing the neutronic parameters and burnup stability of different moderated control rods in the lifetime of the whole reactor, the moderated control rod with the parameter of  $R_m/R \approx 0.5$  achieves a 7% increase in CRW while saving an investment of 30% of B<sub>4</sub>C at BOC. Compared to the complete B<sub>4</sub>C rod, the reactivity loss at the EOC of this design only increases by 2.4%. Designs with other promising absorbing materials would be evaluated in the future.

### 3.3 Control rods with small sized pins

Table 6 shows the criticality calculation results of all the designs with small-sized pins. For control rods with a pure absorber, there are three new designs with 7, 37, and 127 pins. Due to the decrease of the inventory of the absorber, the CRW has slightly decreased, but the efficiency of the control rod is still enhanced (see CRW per unit mass absorber in Table 6). The burnup stability of control rods with different small-sized pins is then evaluated as manifested in Fig. 11. Due to the reduction of the absorber, the reactivity loss of all these designs has increased. At EOC, the CRW of these three control rods has dropped by 18.9%, 32.8%, and 32.4%, respectively.

In the composite control rod designed with absorber and moderator pins, there are two opposite effects: the advantageous one coming from the increasing of the neutronic efficiency due to the moderator and the adverse one resulting in the decrease of the burnup stability due to the reduction of the absorber. As tabulated in Table 6, compared with the design of pure absorber pins, the CRW and neutronic efficiency of the composite control rod has been significantly improved. Among these new composite rods, the efficiency of the design with 37 pins has increased by 25% and that of 127 composite rods has risen by 21%. However, the analysis of the burnup stability of these composite control rods with 7 and 127 pins (see Fig. 12) suggests that their CRW at EOC has decreased accordingly by 4.9% and 6.1%.

In conclusion, both the pure absorber small-sized pins design and the composite control rod with the moderator

**Table 6** Neutronic performance of control rods with small-sized pins

Number of pins	Pin type	$k_{eff}$	$\sigma$	CRW/pcm	CRW per unit mass absorber / (pcm·kg <sup>-1</sup> )	EACS/cm <sup>-1</sup>
1	Absorber pin	1.033	8.0E-05	16300	3.6	1.19E-01
7	All absorber pins	1.056	7.6E-05	14200	4.7	8.21E-02
	6 absorber pins and 1 moderator pin	1.053	7.3E-05	14500	5.6	8.34E-02
37	All absorber pins	1.058	7.5E-05	14000	5.2	8.12E-02
	30 absorber pins and 7 moderator pins	1.056	7.7E-05	14200	6.5	8.27E-02
127	All absorber pins	1.051	7.8E-05	14600	4.8	8.61E-02
	108 absorber pins and 19 moderator pins	1.049	7.5E-05	14900	5.8	8.84E-02

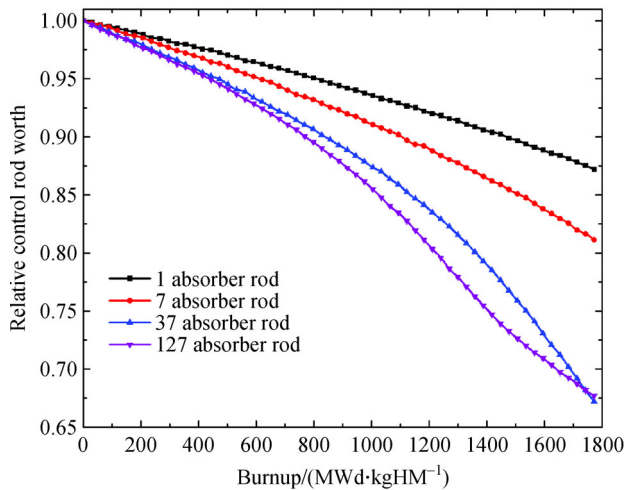


**Fig. 11** Relative CRW changes with burnup for control rod with 1, 7, 37, and 127 absorber pins.

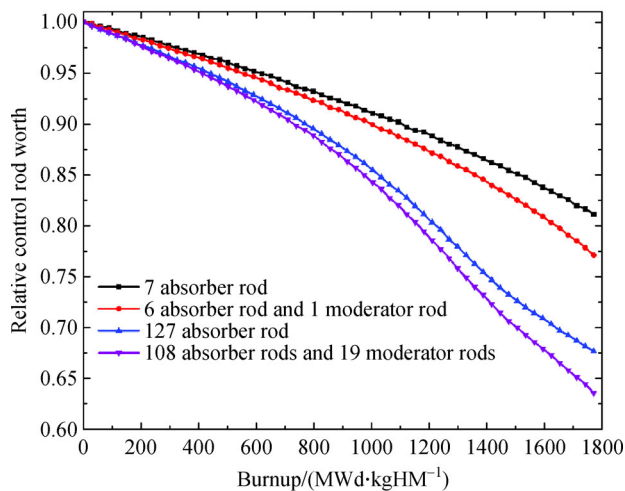


**Fig. 12** Relative CRW changes with burnup for composite control rod using moderator pins.

pins improve the neutronic efficiency. However, all these designs have disadvantages in burnup stability. Compared with the traditional design, there is an average reactivity worth loss of more than 25%. The balance between the increase of neutronic efficiency and the decrease of burnup stability needs further research. Besides, the improvement on safety margin is also nonnegligible.

## 4 Conclusions

In this paper, innovative control rods with the optimized spatial structure are proposed. To assess the performance of these new designs, they are compared with the traditional one concerning the control rod worth, effective absorption cross section, and burnup stability.

Using three promising absorbers including hafnium hydride, dysprosium titanate, and europium oxide, this work first investigated spatially mixed control rods. The characteristics of different absorbers are considered to maximize absorbing properties. The combination of rare-earth absorbers with a long decay chain and  $B_4C$  with a large absorption cross section achieves an average improvement of about three times on the burnup stability. Subsequently, control rods with different proportions of moderator are evaluated. The moderated structure can increase the neutronic efficiency owing to the moderator in the inner region, but excessive moderating may lead to the failure of the control rod. According to the research, the volume ratio of moderator needs to be limited to less than 50%.

To achieve a safer reactivity control, the control rod with more small-sized pins is proposed. This design can provide a higher safety margin by reducing the risk of the control rod failure caused by one rod damage, and the neutronic efficiency can also be improved due to the weaker spatial self-shielding effect. Moreover, the moderator pins are utilized to flatten neutron flux and increase the absorbing capacity of absorber pins around it. However, due to the decrease of the absorber, these two designs both have defects in the burnup stability. In-depth research needs to be further conducted.

In the future, the new configuration of control rods with more promising absorbing materials will be studied for better neutronic performance. Detailed analysis of other characteristics of these absorbers such as conductivity, irradiation resistance, mechanical properties, etc. needs to be implemented. The application of these new designs in other nuclear systems is being conducted.

**Acknowledgements** This work is supported by the National Key R&D Project (Grant No. 2020YFB1901700), and the National Natural Science Foundation of China (Grant No. 11775127).

## References

- Gosset D. Absorber materials for Generation IV reactors. In: Yvon P, ed. *Structural Materials for Generation IV Nuclear Reactors*, Woodhead Publishing 2017
- Onoue M, Kawanishi T, Carlson W R, et al. Application of MSHIM core control strategy for Westinghouse AP1000 nuclear power plant. In: *GENES4/ANP2003*, Kyoto, Japan, 2003
- Safarinia M, Faghihi F, Mirvakili S M, et al. Design of emergency shutdown system for the Tehran Research Reactor, Part I: neutronics investigation. *Annals of Nuclear Energy*, 2017, 103: 306–314
- Guo H, Garcia E, Faure B, et al. Advanced method for neutronic simulation of control rods in sodium fast reactors: numerical and experimental validation. *Annals of Nuclear Energy*, 2019, 129: 90–100
- Park C J, Lee B, Alnajjar A T, et al. Depletion analysis of control absorber in a small research reactor. *Annals of Nuclear Energy*,

- 2013, 60: 377–382
6. Hong L P. Depletion analysis on the control rod absorber of RSG gas oxide and silicide fuel cores. *Atom Indonesia*, 1999, 25(1): 29–46
  7. Horn R M, Frew B D, Van Diemen P. Thermal spectrum control rod materials. In: Konings R J M, Stoller R E, eds. *Comprehensive Nuclear Materials*, Elsevier, 2012
  8. Devan K, Riyas A, Alagan M, et al. A new physics design of control safety rods for prototype fast breeder reactor. *Annals of Nuclear Energy*, 2008, 35(8): 1484–1491
  9. Schunert S, Wang Y, Ortensi J, et al. Control rod treatment for FEM based radiation transport methods. *Annals of Nuclear Energy*, 2019, 127: 293–302
  10. Sakurai F, Horiguchi Y, Kobayashi S, et al. Present status and future prospect of JRR-3 and JRR-4. *Physica B, Condensed Matter*, 2002, 311(1–2): 7–13
  11. Ye C. China Advanced Research Reactor (CARR): a new reactor to be built in China for neutron scattering studies. *Physica B, Condensed Matter*, 1997, 241–243: 48–49
  12. Guo H, Buiron L. Innovative sodium fast reactors control rod design. In: *Atoms for the Future 2018 & 4th GIF Symposium*, Paris, France, 2018
  13. Guo H, Buiron L, Kooyman T, et al. Optimized control rod designs for Generation-IV fast reactors using alternative absorbers and moderators. *Annals of Nuclear Energy*, 2019, 132: 713–722
  14. Guo H, Sciora P, Buiron L, et al. Design directions of optimized reactivity control systems in sodium fast reactors. *Nuclear Engineering and Design*, 2019, 341: 239–247
  15. Čerba Š, Vrban B, Lüley J, et al. Optimization of the heterogeneous GFR 2400 control rod design. *Progress in Nuclear Energy*, 2017, 97: 170–181
  16. Wang K, Li Z, She D, et al. RMC—a Monte Carlo code for reactor core analysis. *Annals of Nuclear Energy*, 2015, 82: 121–129
  17. Goorley T, James M, Booth T, et al. Features of MCNP6. *Annals of Nuclear Energy*, 2016, 87: 772–783
  18. Romano P K, Josey C J, Johnson A E, et al. Depletion capabilities in the OpenMC Monte Carlo particle transport code. *Annals of Nuclear Energy*, 2021, 152: 107989
  19. Leppänen J. Serpent—a continuous-energy Monte Carlo reactor physics burnup calculation code. VTT Technical Research Centre of Finland, 2013, available at the website of [montecarlo.vtt.fi](http://montecarlo.vtt.fi)
  20. Cetnar J, Wallenius J, Gudowski W. MCB: a continuous energy Monte Carlo burnup simulation code. In: *Proceedings of the 5th International Information Exchange Meeting on Actinide and Fission Product Partitioning and Transmutation*, 1999
  21. Okumura K, Mori T, Nakagawa M, et al. Validation of a continuous-energy Monte Carlo burn-up code MVP-BURN and its application to analysis of post irradiation experiment. *Journal of Nuclear Science and Technology*, 2000, 37(2): 128–138
  22. Croff A G. ORIGEN2: a versatile computer code for calculating the nuclide compositions and characteristics of nuclear materials. *Nuclear Technology*, 1983, 62(3): 335–352
  23. She D, Liu Y, Wang K, et al. Development of burnup methods and capabilities in Monte Carlo code RMC. *Annals of Nuclear Energy*, 2013, 51: 289–294
  24. She D, Liang J, Wang K, et al. 2D full-core Monte Carlo pin-by-pin burnup calculations with the RMC code. *Annals of Nuclear Energy*, 2014, 64: 201–205
  25. Wang K, Liu S, Li Z, et al. Analysis of BEAVRS two-cycle benchmark using RMC based on full core detailed model. *Progress in Nuclear Energy*, 2017, 98: 301–312
  26. Blanchet D, Fontaine B. Control rod depletion in sodium-cooled fast reactor: models and impact on reactivity control. *Nuclear Science and Engineering*, 2014, 177(3): 260–274
  27. Collins P E, Luciano N, Maldonado G I. Parametric study to capture the skin effect in PWR control rod depletion. *Transactions of the American Nuclear Society*, 2013, 119: 1327–1329
  28. Isotalo A E, Davidson G G, Pandya T M, et al. Flux renormalization in constant power burnup calculations. *Annals of Nuclear Energy*, 2016, 96: 148–157
  29. Pusa M. Rational approximations to the matrix exponential in burnup calculations. *Nuclear Science and Engineering*, 2011, 169(2): 155–167
  30. Franceschini F, Zhang B, Mayhue L, et al. Development of a control rod depletion methodology for the Westinghouse NEXUS system. *Progress in Nuclear Energy*, 2013, 68: 235–242
  31. Massih A R, Rajala T, Jernkvist L O. Analyses of pellet-cladding mechanical interaction behaviour of different ABB Atom fuel rod designs. *Nuclear Engineering and Design*, 1995, 156(3): 383–391
  32. Iwasaki T, Konashi K. Development of hydride absorber for fast reactor—application of hafnium hydride to control rod of large fast reactor. *Journal of Nuclear Science and Technology*, 2009, 46(8): 874–882
  33. Risovany V D, Varlashova E E, Suslov D N. Dysprosium titanate as an absorber material for control rods. *Journal of Nuclear Materials*, 2000, 281(1): 84–89
  34. Pasto A E. Europium oxide as a potential LMFBR control material. Technical Report, Oak Ridge National Lab, 1973
  35. Shoushtari M K, Kakavand T, Sadat Kiai S M, et al. Monte Carlo simulation of a research reactor with nominal power of 7 MW to design new control safety rods. *Nuclear Instruments & Methods in Physics Research, Section B, Beam Interactions with Materials and Atoms*, 2010, 268(5): 519–523
  36. Fadaei A H, Setayeshi S. Control rod worth calculation for VVER-1000 nuclear reactor using WIMS and CITATION codes. *Progress in Nuclear Energy*, 2009, 51(1): 184–191